$\langle Q(R)\rangle_0$ is correctly calculated for arbitrary i and j; however, the deviation from that limit, which vanishes as $1/N^{1/2}$, is correctly calculated only if i and j are the end beads.

A possible problem occurs in the mechanics of the calculation for $\nu = -1$, depending on the procedures used. The prospective pitfalls can be avoided by taking the limit $\nu \to -1$, from above.

The simplest diagrams lead rather quickly to eq 4.7, and that in turn to eq 4.8. There remains only to record that the integral in eq 4.11 is given by

$$C_\nu = \nu^{-1}\int_0^1 [-9\nu/(2y^{1/2}) + 9(1-y)f_2(y)y^{-5/2} + 3\nu f_1(y)y^{-3/2}]\,dy \quad \text{(A2)}$$

where

$$f_1(y) \equiv (1-y)^{\nu/2} - 1$$

and

$$f_2(y) \equiv -f_1(y) - \nu y/2$$

References and Notes

(1) Yamakawa, H. "Modern Theory of Polymer Solutions"; Harper and Row: New York, 1971.
(2) Schmidt, M.; Burchard, W. *Macromolecules* **1981**, *14*, 210.
(3) Guttman, C. M.; McCrackin, F. L.; Han, C. C. *Macromolecules* **1982**, *15*, 1205.
(4) Fixman, M. *Macromolecules* **1981**, *14*, 1710.
(5) Fixman, M. *J. Chem. Phys.* **1983**, *78*, 1588.
(6) Fixman, M. *J. Chem. Phys.* **1983**, *78*, 1594.
(7) Fixman, M. Work in progress on improved variational bounds to the translational diffusion constant. Simulation results that are believed to provide rather good estimates show a significant dependence on the bead friction constant for chains with ca. 1000 statistical segments.
(8) Rotne, J.; Prager, S. *J. Chem. Phys.* **1969**, *50*, 4831.
(9) Fixman, M. *J. Chem. Phys.* **1982**, *76*, 6124.
(10) Allegra, G. *Macromolecules* **1983**, *16*, 555.
(11) Martin, J. E., private communication.
(12) If the intermolecular distance R_{12} were specified in terms of the distance between any two beads rather than between centers of mass, a sharp dependence on R_{12} would develop at short distances. Our procedure seems similar to that of Olaj and Pelinka (Olaj, O. F.; Pelinka, K. H. *Makromol. Chem.* **1976**, *177*, 3413). However, they used strong potentials and 50-bead chains and obtained qualitatively different results for $F(R)$.
(13) Fixman, M. *J. Chem. Phys.* **1955**, *23*, 1656.

Light Scattering Study on Polystyrene in Cyclohexane below the Θ Point†

Yoshiyuki Einaga, Shigeyuki Ohashi, Zhen Tong, and Hiroshi Fujita*

Department of Macromolecular Science, Osaka University, Toyonaka, Osaka 560, Japan.

Received August 2, 1983

ABSTRACT: Light scattering measurement was performed on three monodisperse polystyrene samples ($M = 10 \times 10^3$, 43.6×10^3, and 180×10^3) in cyclohexane in the temperature range from the theta point Θ to 1 °C above the cloud point. From the data obtained the Flory–Huggins interaction parameter χ was expressed as a function of temperature T, polymer volume fraction ϕ, and molecular weight M. This expression for χ was extended to T below the cloud point to calculate critical points, cloud point curves, and spinodals for a series of M values. Good agreement, certainly better than obtained by previous formulations, was found between the calculated results and some typical experimental data. The success is due primarily to the formulation of the experimental finding that χ at high concentration depends significantly on M, in contrast to the usual concept on thermodynamic behavior of concentrated polymer solutions.

This paper is concerned with a very basic but still less satisfactorily solved problem in polymer solution thermodynamics. It is to establish the Flory–Huggins interaction parameter χ that allows quantitative and consistent prediction of phase relationships in strictly binary solutions consisting of a monodisperse polymer and a pure solvent—the simplest of polymer solutions. Much has been worked out over the past 3 decades to find such an expression. Yet, the results obtained do not seem fully satisfactory.[1] This may be understood from the following brief, but somewhat biased, survey of previous studies which we believe have made substantial contributions to the problem concerned.

In 1970, Koningsveld et al.[2] derived from critical point data for polystyrene in cyclohexane an empirical expression

$$\chi = 0.2035 + 90.65T^{-1} + 0.3092\phi + 0.1554\phi^2 \quad (1)$$

for χ at T below the theta point Θ. Here, T is the absolute temperature and ϕ the volume fraction of the polymer in the solution. It should be noted that eq 1 does not contain the molecular weight M of the polymer as the variable. In 1971, Scholte[3] published an important experimental study in which he determined χ for the polystyrene + cyclohexane system above and below Θ by light scattering and could represent the results in terms of an expression similar to eq 1 but different in that the coefficient of T^{-1} depends on M. Either eq 1 or Scholte's expression was less satisfactory, yielding spinodals significantly narrower than the observed ones.

In a paper also of 1971, Koningsveld and Kleintjens[4] reanalyzed the above-mentioned critical point data, assuming for χ a closed expression as

$$\chi = \alpha + (\beta_{00} + \beta_{01}T^{-1})(1-\gamma)/(1-\gamma\phi)^2 \quad (2)$$

where α, β_{00}, β_{01}, and γ are constants. This approach, however, failed to achieve consistent agreement with observed spinodals for different molecular weight samples.

It became evident from these studies that χ depends on M as well as on T and ϕ and that an M dependence must be taken into χ for an accurate prediction of binodals and spinodals of polymer solutions. An interesting theory in this line of thought was presented by Koningsveld et al.[5] in 1974. Considering the well-known fact that the spatial

† It is our great pleasure to dedicate this paper to Professor W. H. Stockmayer on occasion of his 70th birthday.

0024-9297/84/2217-0527$01.50/0

distribution of polymer segments in a solution is inherently nonuniform at low concentrations and becomes uniform at sufficiently high concentrations, these authors proposed to write χ as

$$\chi = Q\chi_{dil} + (1 - Q)\chi_{conc} \quad (3)$$

Here, χ_{dil} and χ_{conc} denote the χ functions characterizing dilute and concentrated solutions, respectively, and Q denotes the probability that a small volume element in the solution is not pervaded by any polymer segments. In actual calculations, the χ function predicted by the two-parameter theory of dilute polymer solutions was substituted for χ_{dil} and the χ function of Koningsveld and Kleintjens (eq 2) for χ_{conc}. Further, it was assumed that Q decays exponentially with ϕ at a rate proportional to $M^{1/2}$. It should be noted that, in this "hybrid" approach, χ depended on M through the terms χ_{dil} and Q. In fact, a fairly good agreement was obtained between calculated and measured spinodal temperatures when the parameter governing the exponential decay of Q was properly adjusted. To date, however, no corresponding comparison has been published with respect to binodal temperature.

Recently, Fujita and Teramoto[6] have described a different approach to the determination of χ for strictly binary polymer solutions. Assuming that eq 1 is valid at any T in regard to the concentration dependence of χ, they estimated the temperature dependence of χ at T below T_c (the critical temperature) from the phase equilibrium relation for the solvent component combined with cloud point data. The χ function so obtained for the polystyrene + cyclohexane system yielded spinodals fitting closely experimental data over a wide range of M. It also yielded good agreement between calculated and experimental binodals (unpublished[7]). Nonetheless, as Helfand[8] criticized, Fujita and Teramoto's approach is debatable, since it predicts such physically anomalous behavior that the temperature coefficient of χ changes discontinuously at $T = T_c$.

Direct measurement of χ is not feasible in the region of T and ϕ where phase separation takes place. Hence, χ in this region must be estimated by extrapolating the data on one-phase solutions. Critical tests of the extrapolated χ may be made by comparing the critical points, binodals, and spinodals calculated therefrom with accurate experimental data of these quantities. It is crucial for an accurate extrapolation to measure χ precisely down to a temperature as close to the cloud point as possible. However, few experimental data meeting this requirement have been published to date.

In this work, light scattering determination of χ down to about 1 °C above the cloud point was undertaken on three monodisperse polystyrene samples in cyclohexane. The molecular weight dependence of χ was inferred from the data obtained, and an empirical expression representing χ as a function of T, ϕ, and M was derived. With this expression, χ below the cloud point was extrapolated to calculate critical points, binodals, and spinodals and the results were compared with typical experimental data.

Experimental Section

Polystyrene Samples. Standard polystyrene samples F1, F4, and F20, so designated by the supplier Toyo Soda Co., were divided into several fractions by fractional precipitation using the benzene + methanol system to sharpen further their already sufficiently narrow molecular weight distributions. The main fractions of F20 were further fractionated by the column elution method. In this way, three samples designated as f1 (from F1), f4 (from F4), and f18 (from F20) were prepared for the present work. GPC measurements confirmed very narrow molecular weight distributions of these samples.

The weight-average molecular weight M_w was 10 000, 43 600, and 180 000 for the samples f1, f4, and f18, respectively. These were obtained by light scattering in benzene at 25 °C, using the procedures established in this laboratory.

Light Scattering Measurements. Intensities of light scattered by polystyrene + cyclohexane solutions were measured at angles between 30 and 150° in the range of polymer volume fraction ϕ (see below for the definition of ϕ) from 0.02 to 0.2 for f1, from 0.01 to 0.225 for f4, and from 0.01 to 0.13 for f18. A Fica 50 light scattering photometer was used with polarized incident light of 546.1-nm wavelength. At each concentration the measuring temperature was lowered at appropriate intervals from 34.5 °C (Θ) to a value about 1 °C above the cloud point: 34.5 → 10 °C for f1, 34.5 → 15 °C for f4, and 34.5 → 24 °C for f18, each maintained to within 0.05 °C. Neutral-density filters were inserted when scattering intensities were too high. Either a polystyrene + xylene solution or a glass block was used as the working standard to determine transmittance of the filters and also to check the stability of the apparatus.

The light scattering data were analyzed by using the well-known relation[9] for the excess Rayleigh ratio ΔR_0 at the zero scattering angle:

$$K/\Delta R_0 = -(1/RT\phi)(\partial\Delta\mu_0/\partial\phi)_{T,p} \quad (4)$$

where

$$K = (4\pi^2n^2/N_A\lambda_0^4)(\partial n/\partial\phi)^2V_0 \quad (5)$$

Here, $\Delta\mu_0$ is the excess chemical potential of the solvent, R the gas constant, n the refractive index of the solution, N_A the Avogadro constant, λ_0 the wavelength of the incident light, V_0 the molar volume of the solvent, and $\partial n/\partial\phi$ the refractive index increment. Values of $\partial n/\partial\phi$ at various temperatures and concentrations were computed by utilizing Scholte's equation[9,11] relevant to the present system:

$$\partial n/\partial w = n_0(T) + 0.070w + 0.058w^2 \quad (6)$$

with

$$n_0(T) = (693.7 + 2T) \times 10^{-4} \quad (7)$$

where the polymer weight fraction w is related to ϕ by[11]

$$\phi = [1 + (V_0/M_0v_p)(w^{-1} - 1)]^{-1} \quad (8)$$

with M_0 the molecular weight of the solvent and v_p the partial specific volume of the polymer. We used 108.76 cm^3/mol for V_0 and 0.9343 cm^3/g for v_p, each referring to 25 °C.

Preparation of Solutions. A given polymer sample was dissolved in benzene and repeatedly filtered through Millipore membranes until scattering from dust particles became undetectable by visual observation of the laser beam passing through the solution. The filtered solution was then freeze-dried in a vessel covered with a Millipore film. A proper amount of the dry polymer was placed in a cylindrical light scattering cell provided with a ground-glass stopper and again dried to remove traces of moisture. Carefully rectified cyclohexane was then poured into the cell in a drybag filled with nitrogen, and the cell was sealed. Great care was taken to prevent the test solution from being phase separated prior to each light scattering measurement.

The polymer weight fraction w was calculated from the weights of the polymer and solvent used, and the polymer volume fraction ϕ was then evaluated by eq 8.

Results

Experimental Data. Figure 1 depicts the angular dependence of K/R_θ for sample f4 at two largely different concentrations. The high-concentration data at each temperature in Figure 1a can be fitted by a straight line and extrapolated to the zero scattering angle to evaluate $K/\Delta R_0$ accurately. The low-concentration data in Figure 1b also follow a straight line for temperatures higher than 25 °C but begin deviating downward at small scattering angles when the temperature is lowered below 25 °C. The deviations become progressively more pronounced with

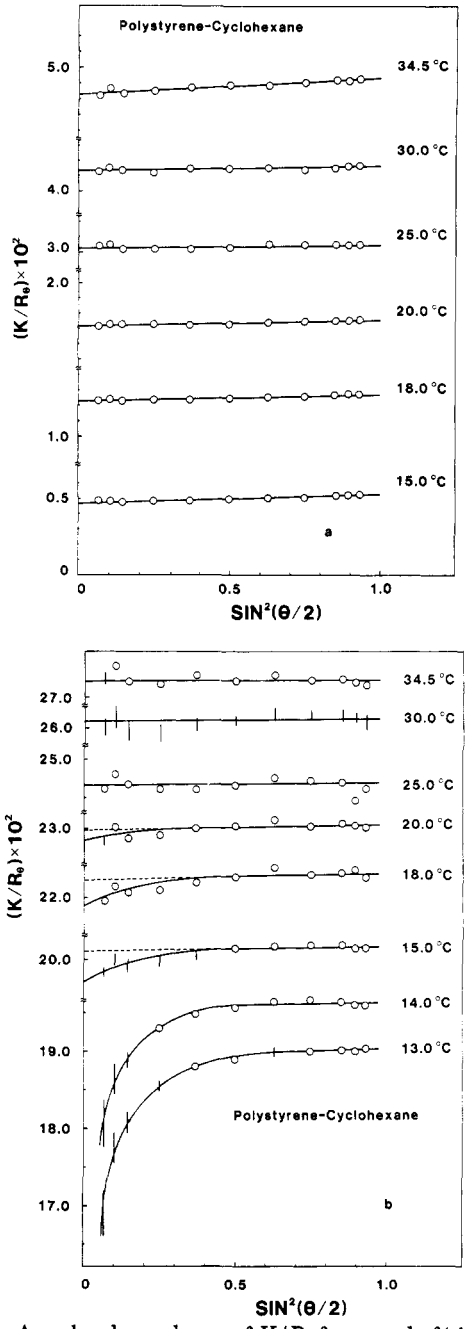

Figure 1. Angular dependence of K/R_θ for sample f4 in cyclohexane at the temperatures indicated. The values of ϕ in parts a and b are 0.07008 and 0.009902, respectively.

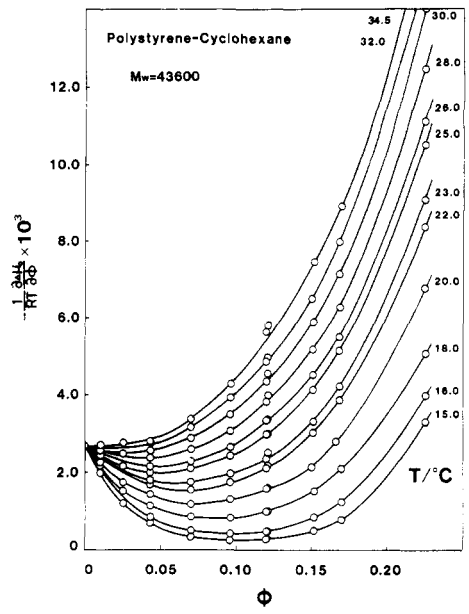

Figure 2. Concentration dependence of $-(1/RT)(\partial\Delta\mu_0/\partial\phi)$ for sample f4 in cyclohexane at the temperatures indicated.

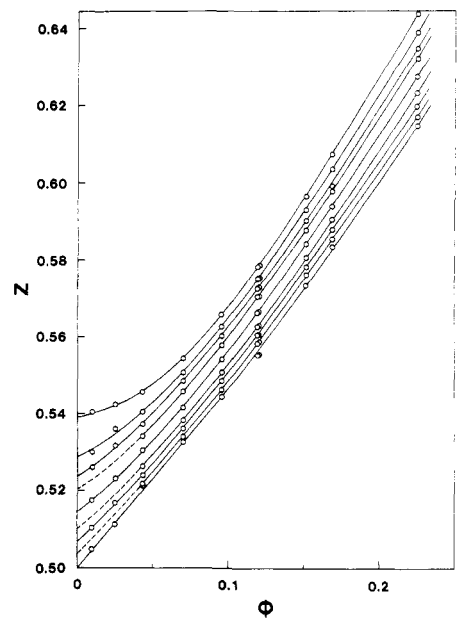

Figure 3. Plots of Z vs. ϕ for sample f4. The temperature is 15, 18, 20, 22, 25, 28, 30, 32, and 34.5 °C from top to bottom.

decreasing temperature and approaching cloud point. This phenomenon probably reflects the occurrence of microphase separation, which triggers macroscopic phase separation of the solution. Because of these deviations the K/R_θ data for temperatures below 15 °C in Figure 1b were discarded and those at 15, 18, and 20 °C were extrapolated to the zero angle as indicated by the dashed lines.

Figure 2 shows the ϕ dependence of $-(1/RT)(\partial\Delta\mu_0/\partial\phi)$ for sample f4 calculated by substituting $K/\Delta R_0$ data into eq 4. It can be seen that at 34.5 °C, $-(1/RT)(\partial\Delta\mu_0/\partial\phi)$ remains almost constant for relatively small ϕ and then increases rapidly with ϕ. At lower temperatures, $-(1/RT)/(\partial\Delta\mu_0/\partial\phi)$ decreases initially, passes through a minimum, and increases monotonically with increasing ϕ. The common ordinate intercept of these curves gives the reciprocal relative chain length P^{-1} of the sample. Here, P is defined by

$$P = (v_p/V_0)M \tag{9}$$

The P value obtained in this way was 86.0, 375, and 1550 for samples f1, f4, and f18, respectively.

The initial slope of each curve in Figure 2 gives $2(V_0/v_p)A_2$, where A_2 is the second virial coefficient of the system. Thus we find for sample f4 that A_2 is essentially zero at 34.5 °C, as expected, and decreases monotonically with decreasing temperature. The curves of Figure 2 also indicate that $-(1/RT)(\partial\Delta\mu_0/\partial\phi)$ at fixed ϕ decreases almost linearly with increasing T^{-1}. This behavior allows us to estimate with fair accuracy spinodal temperatures at which $-(1/RT)(\partial\Delta\mu_0/\partial\phi)$ vanishes.

Interaction Parameter. Substitution of the Flory–Huggins equation for $\Delta\mu_0$ into eq 4 gives

$$Z = \chi + (1/2)(\partial\chi/\partial\phi)\phi = [1/(1-\phi) + 1/P\phi - K/\Delta R_0]/2 \tag{10}$$

Since all the quantities appearing in the last term of eq 10 are experimentally measurable, light scattering measurement permits one to evaluate the parameter Z, but not χ itself.

Figure 3 depicts the Z vs. ϕ plot for sample f4. Those for samples f1 and f18 were similar to this and hence are not shown here. The following features may be noted from Figure 3: (1) At relatively high concentrations, i.e., $\phi > 0.1$, Z at a fixed temperature increases with ϕ following a smooth curve slightly bent upward. (2) The Z curves for different temperatures are approximately parallel and their average slopes are not very different from 0.5 in the range of ϕ indicated. (3) In the region of high dilution, the Z curve begins to deviate upward from the smooth extension of its high-concentration branch when the temperature is lowered a few degrees below 34.5 °C, the Θ temperature of this polymer + solvent system. The upward bending becomes more pronounced with decreasing temperature.

Data Analysis

Hybrid Theory. Equation 3 may be rewritten

$$\chi(T,\phi;P) = \chi_{conc}(T,\phi;P) + [\chi_{dil}(T,\phi;P) - \chi_{conc}(T,\phi;P)]Q(T,\phi;P) \quad (11)$$

Following Koningsveld et al.[5] we approximate the terms χ_{dil} and χ_{conc} in the brackets by their infinite-dilution values $\chi^0_{dil}(T;P)$ and $\chi^0_{conc}(T;P)$ and assume Q to vary only with ϕ/ϕ^*. Here, ϕ^* is the so-called overlap concentration and may be represented by

$$\phi^* = DP^{-1/2} \quad (12)$$

with D being a parameter characteristic of the system under study. Unlike Koningsveld et al.,[5] we make no assumption for $Q(\phi/\phi^*)$, but it is worthwhile to note that mathematically Q approaches unity as $\phi \to 0$ and physically should decrease monotonically to zero with increasing ϕ.

Substituting eq 11 into eq 10 and using the approximations introduced above, we obtain

$$Z(T,\phi;P) = Z_{conc}(T,\phi;P) + [\chi^0_{dil}(T;P) - \chi^0_{conc}(T;P)]R(\phi/\phi^*) \quad (13)$$

where

$$Z_{conc} = \chi_{conc} + (1/2)(\partial\chi_{conc}/\partial\phi)_T\phi \quad (14)$$

$$R(\phi/\phi^*) = Q(\phi/\phi^*) + (1/2)(\phi/\phi^*)\, dQ(\phi/\phi^*)/d(\phi/\phi^*) \quad (15)$$

It follows from eq 14 that

$$\lim_{\phi\to 0} Z_{conc} = \chi^0_{conc}(T;P) \quad (16)$$

Thus, when $Z_{conc}(T,\phi;P)$ is expressed as a function of ϕ, its ϕ-independent term can be written $\chi^0_{conc}(T;P)$. This quantity is treated as a parameter in the subsequent development, since its physical meaning is not always clear. We also note that $R(\phi/\phi^*)$ tends to unity as ϕ approaches zero. With these properties, it follows from eq 13 that

$$\lim_{\phi\to 0} Z = \chi^0_{dil}(T;P) \quad (17)$$

Hence, χ^0_{dil} in eq 13 may be estimated by extrapolating Z vs. ϕ plots to infinite dilution. In contrast to χ^0_{conc}, this quantity has a definite physical meaning that $0.5 - \chi^0_{dil}$ varies linearly with the second virial coefficient of the system, with a proportionality coefficient essentially independent of P.[1]

When, as in the present analysis, no a priori assumption is made for the form of $Q(\phi/\phi^*)$ and hence of $R(\phi/\phi^*)$, there is no unique way of resolving measured Z into the "concentrated-solution" term Z_{conc} and the "dilute-solution" correction $Z_{dil} = (\chi^0_{dil} - \chi^0_{conc})R(\phi/\phi^*)$. This difficulty is the most unfavorable aspect of Koningsveld et al.'s hybrid theory.[5] In this work, we attempted to resolution invoking a working hypothesis which we believe seems reasonable. The actual process followed is illustrated below with the Z data for sample f4.

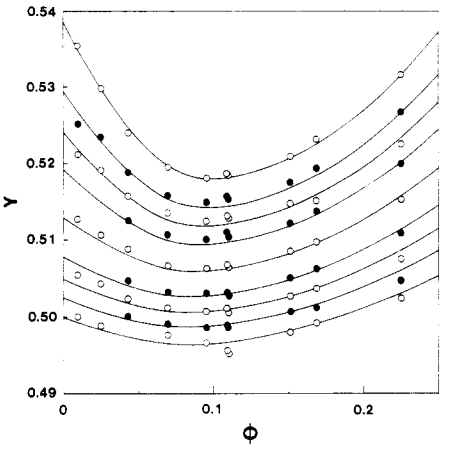

Figure 4. Plots of Y vs. ϕ for sample f4. The temperature is 15, 18, 20, 22, 25, 28, 30, 32, and 34.5 °C from top to bottom. Solid lines indicate the calculated values (see text for details).

Expression of Z for Sample f4. Because of the above-mentioned feature (2) of our experimental Z vs. ϕ plots, it is advantageous to express Z_{conc} as

$$Z_{conc}(T,\phi;P) = \chi^0_{conc}(T;P) + (1/2)\phi + f(T,\phi;P) \quad (18)$$

and determine $f(T,\phi;P)$ from Z data at high concentrations. Substituting eq 18 into eq 13 and introducing Y defined as

$$Y = Z - (1/2)\phi \quad (19)$$

we obtain

$$Y(T,\phi;P) = Y_{dil}(T,\phi;P) + Y_{conc}(T,\phi;P) \quad (20)$$

where $Y_{dil}(T,\phi;P)$ and $Y_{conc}(T,\phi;P)$ are defined, respectively, by

$$Y_{dil}(T,\phi;P) = [\chi^0_{dil}(T;P) - \chi^0_{conc}(T;P)]R(\phi/\phi^*) \quad (21)$$

$$Y_{conc}(T,\phi;P) = \chi^0_{conc}(T;P) + f(T,\phi;P) \quad (22)$$

Figure 4 illustrates Y vs. ϕ plots for sample f4. It is seen that Y exhibits a minimum at any T indicated and that the minima at different T are all located at the concentrations near $\phi = 0.1$. This behavior of Y suggests that Y consists of two functions of ϕ, one decreasing and the other increasing monotonically with ϕ. It is reasonable to assign the former to Y_{dil}, in view of the above-mentioned property of the function $R(\phi/\phi^*)$. Thus, the latter is here taken to be Y_{conc}.

The most serious question is the extent to which Y_{dil} stretches to the region beyond the minima, but no definite information is yet available for answering it. Therefore, we here make an ad hoc assumption that Y_{dil} sharply diminishes to zero in the vicinity of each minimum point. This is equivalent to considering that the Y data for $\phi > 0.1$ in Figure 4 represent the behavior of Y_{conc}. Such assignment of Y_{conc} is simply a working hypothesis at the present stage of our knowledge.

After several trials we found that an empirical equation

$$Y_{conc}(T,\phi;P_4) = \chi^0_{conc}(T;P_4) + 10\phi^4/[1 + b(T;P_4)\phi^2] \quad (23)$$

yields a close fit to $Y(T,\phi;P)$ for $\phi > 0.12$ if appropriate values are assigned to $\chi^0_{conc}(T;P_4)$ and $b(T;P_4)$ for different T, where P_4 is the P value of sample f4. The best-fit values

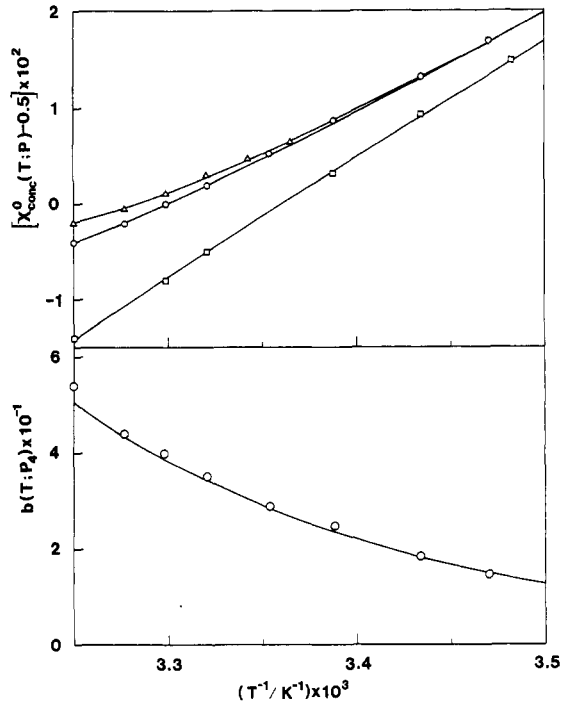

Figure 5. Parameters $\chi^0_{conc}(T;P)$ (upper panel) and $b(T;P_4)$ (lower panel) plotted against T^{-1}. Various marks signify different samples: circles, f4; squares, f1; and triangles, f18. Solid lines were calculated by eq 31 for χ^0_{conc} and eq 24 for $b(T;P_4)$.

of these parameters are shown by circular marks in Figure 5. The lines fitting these marks are represented by

$$b(T;P_4) = 50.5 \exp[-18(\Theta/T - 1)] \quad (24)$$

$$\chi^0_{conc}(T;P_4) = 0.4930 + 0.345(\Theta/T - 1) + 0.0029 \exp[-30(\Theta/T - 1)] \quad (25)^{12}$$

where Θ, the theta temperature of the system under study, is taken to be 307.65 K (34.5 °C). Reference is made later to the triangular and square marks along with the lines fitting them in Figure 5.

By putting measured Y values and those of $Y_{conc}(T,\phi;P_4)$ calculated from eq 23, 24, and 25 into eq 20, $Y_{dil}(T,\phi;P_4)$ was computed and then divided by $\chi^0_{dil}(T;P_4) - \chi^0_{conc}(T;P_4)$. In so doing, eq 27, rather than extrapolated Z (see eq 17), was used for estimating $\chi^0_{dil}(T;P_4)$. When the resulting R values for different T were plotted against ϕ, the data points fell approximately on a single curve. As the best-fit line we chose one represented by

$$R = \exp(-20\phi - 2150\phi^3) \quad (26)$$

The solid lines in Figure 4 show the behavior of $Y(T,\phi;P_4)$ calculated with eq 23 for Y_{conc} and eq 26 for R. Their fit to data points may be considered satisfactory, since the measuring accuracy of Y is ±0.0005 at best.

Generalization. The next step is to incorporate the variable P in the expressions for $Y_{dil}(T,\phi;P_4)$ and $Y_{conc}(T,\varphi;P_4)$, using the Z data on samples other than f4. Because of the very limited data available here, this operation inevitably involves a series of guess work.

A. P Dependence of χ^0_{dil}. Our recent light scattering experiment led to an interesting finding that the second virial coefficient A_2 or equivalently the quantity χ^0_{dil} for monodisperse polystyrene in cyclohexane below Θ is essentially independent of P, at least in the range of T and P studied.[13] This is illustrated in Figure 6, where the data points include five samples ranging in M from 1×10^4 to 50×10^4. The line drawn in the figure represents

$$\chi^0_{dil}(T) = 0.5 + 0.26(\Theta/T - 1) + 4.6(\Theta/T - 1)^2 \quad (27)$$

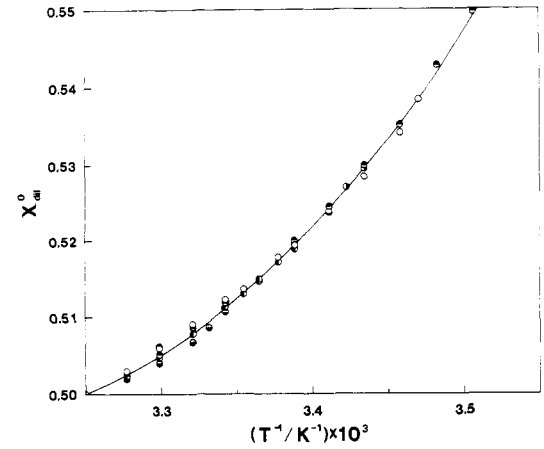

Figure 6. Parameter χ^0_{dil} plotted against T^{-1} for samples of different molecular weight indicated by different marks: (●) 10000 (f1); (○) 43600 (f4); (◑) 73700; (◐) 180000 (f18); (◒) 498000. The solid line was calculated by eq 27.

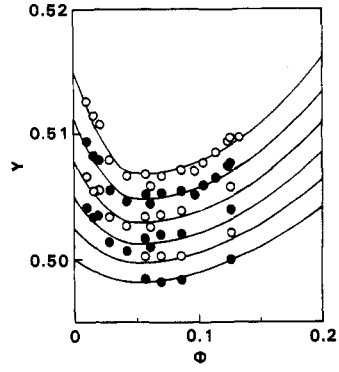

Figure 7. Plots of Y vs. ϕ for sample f18. The temperature is 24, 26, 28, 30, 32, and 34.5 °C from top to bottom. Solid lines indicate the calculated values (see text for details).

Here, the variable P has been taken out of $\chi^0_{dil}(T;P)$ to signify the condition that χ^0_{dil} does not depend on P. In the ensuing analysis, eq 27 is used for calculating χ^0_{dil} at any temperature either above or below the cloud point. It should be noted that eq 27 gives 0.26 for $[d\chi^0_{dil}/d(\Theta/T)]_{T=\Theta}$, which is consistent with the value 0.25 deduced for this "initial" slope using Miyaki and Fujita's results for the binary cluster integral above Θ.[14]

B. P Dependence of R. If, as has been assumed at the beginning of this data analysis, R depends only on ϕ/ϕ^* and ϕ^* varies linearly with $P^{-1/2}$, it follows that $R(\phi/\phi^*)$ is a function of a single combined variable $P^{1/2}\phi$. If this function is forced to agree with eq 26 for $P = P_4$, we obtain for any P

$$R(\phi/\phi^*) = \exp(-P^{1/2}\phi - 0.3P^{3/2}\phi^3) \quad (28)$$

In what follows, we assume that this equation is applicable to any P. If this assumption is valid, it turns that the "dilute-solution" correction vanishes at a lower concentration as P becomes larger.

C. P Dependence of Y_{conc}. Figure 7 shows Y vs. ϕ plots for sample f18. These plots are similar in overall feature to those for sample f4 (Figure 4). The minima of Y here appear at concentrations lower than those in Figure 4, as expected from the above-mentioned P dependence of the function $R(\phi/\phi^*)$. Comparison of Figures 4 and 7 reveals a more important difference: the behavior of Y beyond the minima, i.e., Y_{conc} according to our interpretation, in Figure 7 cannot be described by eq 23 for $Y_{conc}(T,\phi;P_4)$. This finding implies that Y_{conc} depends on P. A numerical adjustment of the term χ^0_{conc} is not enough to account for this P dependence.

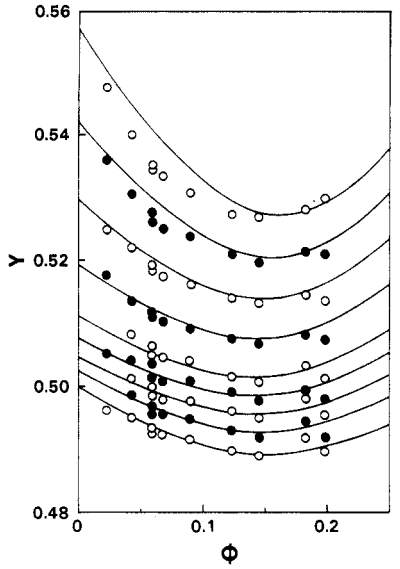

Figure 8. Plots of Y vs. ϕ for sample f1. The temperature is 10, 14, 18, 22, 26, 28, 30, 32, and 34.5 °C from top to bottom. Solid lines indicate the calculated values (see text for details).

After some trials, it was found that $Y_{conc}(T,\phi;P_{18})$ (P_{18} is the value of P for sample f18) can be adequately described by

$$Y_{conc}(T,\phi;P_{18}) = \chi^0_{conc}(T;P_{18}) + 10C\phi^4/[1 + b(T;P_4)C\phi^2] \quad (29)$$

if C is taken to be 1.60 and $\chi^0_{conc}(T;P_{18})$ is chosen properly depending on T. The solid curves in Figure 7 show the Y vs. ϕ relations calculated with eq 28 for $R(\phi/\phi^*)$ and eq 29 for $Y_{conc}(T,\phi;P_{18})$. The chosen values of $\chi^0_{conc}(T;P_{18})$ are plotted as triangular points in the uper panel of Figure 5. The fit of the solid lines to data points in Figure 7 is not as good as in Figure 4 but may be regarded as encouraging.

On the basis of this result and hint by the fact that the chosen value of C (1.60) happened to equal $(P_{18}/P_4)^{1/3}$, we boldly hypothesized that $Y_{conc}(T,\phi;P)$ for any P could be expressed by

$$Y_{conc}(T,\phi;P) = \chi^0_{conc}(T;P) + 10(P/P_4)^{1/3}\phi^4/[1 + b(T;P_4)(P/P_4)^{1/3}\phi^2] \quad (30)$$

with $\chi^0_{conc}(T;P)$ as an adjustable parameter, and proceeded to test the hypothesis with the Y data for sample f1.

The Y vs. ϕ plots for sample f1 are depicted in Figure 8. It is seen that the experimental data do not sufficiently stretch to the concentration region beyond the minima. Hence, these data are not useful for a straightforward testing of eq 30. However, this does not matter for the moment. The expression for $Y(T,\phi;P_1)$ (P_1 is the value of P for sample f1) obtained with eq 28 for $R(\phi/\phi^*)$ and eq 30 for $Y_{conc}(T,\phi;P_1)$ contain only one adjustable parameter $\chi^0_{conc}(T;P_1)$. Trial-and-error operations were carried out to find $\chi^0_{conc}(T;P_1)$ which allows this expression to fit the plotted points in Figure 8. The solid lines in this figure illustrate the best fit we could make. The chosen values of $\chi^0_{conc}(T;P_1)$ are shown by square marks in the upper panel of Figure 5. Except for the two lowest temperatures, the agreement between calculated and measured Y is as good as that seen in Figure 7. The appreciable disagreement in the low-concentration region at 10 °C indicates that $R(\phi/\phi^*)$ given by eq 28 ceases to be adequate at such low temperatures.

In Figure 5, we now have three sets of $\chi^0_{conc}(T;P)$ data. Our final task is to infer the T and P dependence of χ^0_{conc} from this limited information. For this purpose we tried to modify eq 25 and found that an empirical expression

$$\chi^0_{conc}(T;P) = 0.4930 + 0.345(\Theta/T - 1) + (-0.075P^{-1/2} - 45P^{-2} + 0.0070)\exp[-(40 - 520P^{-2/3})(\Theta/T - 1)] \quad (31)$$

fits the three sets of data equally well. The three solid lines in the upper panel of Figure 5 confirm this finding. In what follows, we assume that eq 31 is applicable to any T and P.

D. Proposed Expressions for $Z(T,\phi;P)$ and $\chi(T,\phi;P)$. For convenience of the ensuing discussion we summarize here the important relations deduced from the above data analysis.

Our proposed expression for $Z(T,\phi;P)$ is written

$$Z(T,\phi;P) = \chi^0_{conc}(T;P) + (1/2)\phi + A(P)\phi^4/[1 + B(T;P)\phi^2] + [\chi^0_{dil}(T) - \chi^0_{conc}(T;P)]R(P^{1/2}\phi) \quad (32)$$

where $\chi^0_{conc}(T;P)$, $\chi^0_{dil}(T)$, and $R(\phi/\phi^*)$ are given by eq 31, 27, and 28, respectively, and $A(P)$ and $B(T;P)$ are defined by

$$A(P) = 1.4P^{1/3}$$

$$B(T;P) = 7P^{1/3}\exp[-18(\Theta/T - 1)] \quad (33)$$

The sum of the first three terms on the right-hand side of eq 32 represents the "concentrated-solution" term Z_{conc} and the last term the "dilute-solution" correction Z_{dil}. It is important to note that Z_{conc} depends on P, in contrast to the usual notion that thermodynamic behavior of concentrated polymer solutions should be essentially independent of the molecular weight of the dissolved polymer.

The definition of Z given by eq 10 allows χ to be expressed in terms of Z as

$$\chi = (2/\phi^2)\int_0^\phi Z\phi\, d\phi \quad (34)$$

Substitution of eq 32 into this relation yields

$$\chi(T,\phi;P) = \chi^0_{conc}(T;P) + (1/3)\phi + [A(P)/B(T;P)]\{\phi^2/2 - 1/B(T;P) + \ln[1 + B(T;P)\phi^2]/B(T;P)^2\phi^2\} + [\chi^0_{dil}(T) - \chi^0_{conc}(T;P)]Q(P^{1/2}\phi) \quad (35)$$

with

$$Q(x) = (0.754/x^2)[1 - (1 + 1.875x + 0.864x^2 + 0.525x^3)\exp(-1.875x - 0.432x^2 - 0.175x^3)] \quad (36)$$

Actually, eq 36 is an analytical fit to the numerically evaluated $(2/x^2)\int_0^x R(x)x\, dx$, with errors less than 0.5%.

Discussion

Our expressions for Z and χ were formulated on the basis of experimental information on one-phase solutions. The question is whether they are capable of predicting observed critical points, cloud points, and spinodal temperatures with a satisfactory accuracy when extended smoothly to the region where phase separation takes place. This question should provide critical tests of the proposed expressions, since, as is well-known, phase equilibria of polymer solutions are very sensitive to the form of χ as a function of T, ϕ, and P.

Critical Points. The critical temperature T_c and concentration ϕ_c for a strictly binary solution consisting of a pure liquid and a monodisperse polymer with a relative chain length P can be determined from the set of relations[1]

$$1/(1 - \phi_c) + 1/(P\phi_c) = 2Z_c \quad (37)$$

$$1/(1 - \phi_c)^2 - 1/(P\phi_c^2) = 2(\partial Z/\partial\phi)_c \quad (38)$$

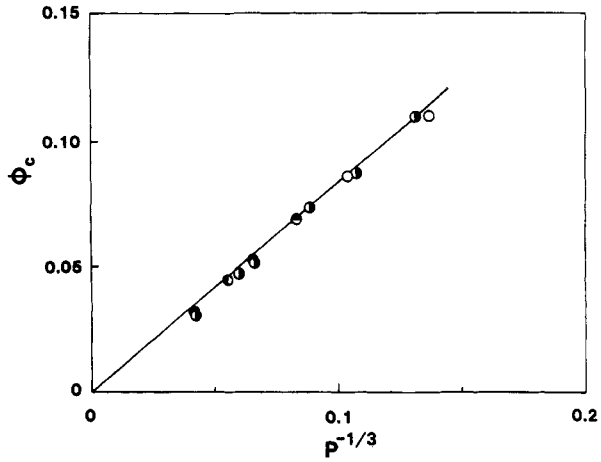

Figure 9. Critical concentration ϕ_c plotted against $P^{-1/3}$ for narrow-distribution polystyrene samples in cyclohexane: (○) Hashizume et al.;[18] (◑) Koningsveld et al.;[2] (●) Kuwahara et al.;[15] (⊖) Nakata et al.[16,17] The solid line was calculated from eq 39 and 40.

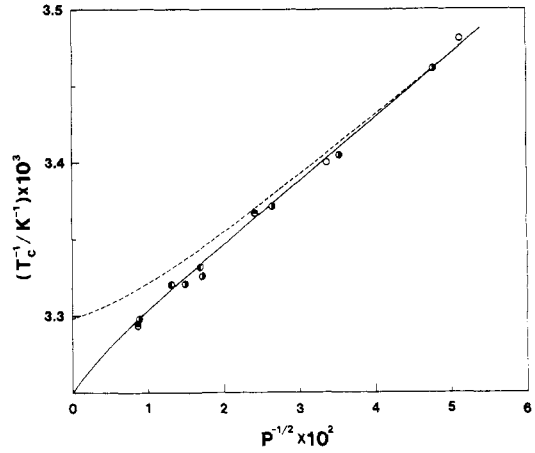

Figure 10. Reciprocal critical temperature T_c^{-1} plotted against $P^{-1/2}$ for narrow-distribution polystyrene samples in cyclohexane. The indicated marks have the same meaning as in Figure 9. Solid and dashed lines were calculated from eq 39 and 40, using molecular-weight-dependent and -independent Y^0_{conc}, respectively (see text for details).

where the subscript c signifies the value at the critical point. Substitution of eq 32 yields

$$\phi_c^2/2(1-\phi_c) + 1/(2P\phi_c) = \chi^0_{conc}(T_c;P) - 1/2 + A(P)\phi_c^4/[1 + B(T_c;P)\phi_c^2] + [\chi^0_{dil}(T_c) - \chi^0_{conc}(T_c;P)]R(P^{1/2}\phi_c) \quad (39)$$

$$\phi_c(2-\phi_c)/2(1-\phi_c)^2 - 1/(2P\phi_c^2) = 2[2 + B(T_c;P)\phi_c^2]\phi_c^3/[1 + B(T_c;P)\phi_c^2]^2 - P^{1/2}[\chi^0_{dil}(T_c) - \chi^0_{conc}(T_c;P)](1 + 0.9P\phi_c^2)R(P^{1/2}\phi_c) \quad (40)$$

Note that these relations contain no adjustable parameter.

The solid lines in Figures 9 and 10 show computed ϕ_c and T_c^{-1} plotted against $P^{-1/3}$ and $P^{-1/2}$, respectively, and various circles indicate experimental data taken from the literature[2,15-17] or determined in our laboratory.[18] For both ϕ_c and T_c, favorable agreement is seen between calculated and measured values over the entire range of P examined. Deviations are less than ±0.005 for ϕ_c and ±0.5 °C for T_c, which may well be compared with uncertainties in the experimental determination of these quantities.

If we had performed the experiment only on a single sample, say f4, and believed in the concept that thermodynamic properties of concentrated polymer solutions

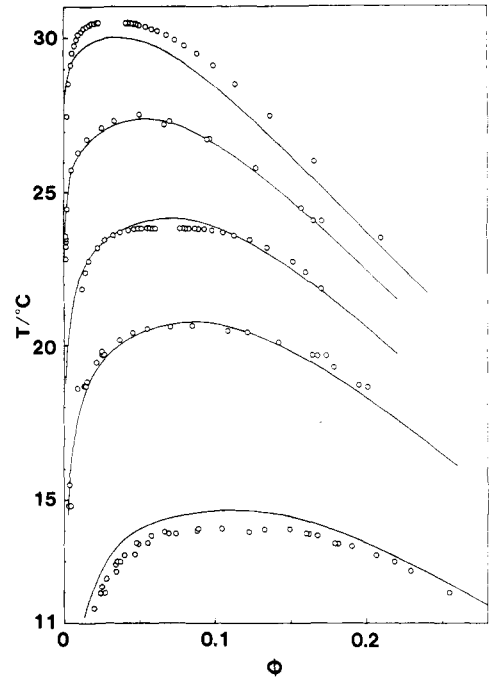

Figure 11. Cloud point curves (binodals) for narrow-distribution polystyrene in cyclohexane. Molecular weights of the samples are 1 560 000 (Nakata et al.[17]), 498 000 (Tsuyumoto et al.[19]), 200 000 (Nakata et al.[16]), 103 000 (Hashizume et al.[18]), and 45 300 (Hashizume et al.[18]) from top to bottom. Solid lines show the results from the present calculation.

should be essentially independent of P, we would have taken $Y_{conc}(T,\phi;P_4)$ to be valid for any P and used it for calculating T_c and ϕ_c as a function of P. The dashed line in Figure 10 illustrates the result obtained by such operation, giving T_c lower than those determined experimentally or estimated from the indicated solid curve. The deviations are greater for larger P, and at the limit of infinite P the dashed line yields a T_c of about 30.0 °C, which is 4.5 °C lower than the Θ temperature of the system under study. This limiting behavior of the dashed line is associated with the fact that, as can be seen from Figure 5, $\chi^0_{conc}(T;P_4) - 0.5$ vanishes at T = 30.0 °C. At any rate, the dashed line illustrates how subtly T_c is affected by the dependence of Y_{conc} or χ_{conc} on P. Though details are not shown here, ϕ_c is sensitive to the concentration dependence of χ itself.

Binodals (Cloud Point Curves). Equation 35 for $\chi(T,\phi;P)$ was substituted in the phase equilibrium relations for the solvent and the polymer, and binodals were calculated for several values of P. The results are depicted as solid lines in Figure 11, where the cloud point data obtained by Nakata et al.[16,17] and in our laboratory[18,19] are included for comparison.

It can be seen that the calculated binodals give miscibility gaps quite favorably compared to the experimental results. The difference between calculated and measured cloud points is less than 1 °C in the ranges of ϕ and P indicated. At the present stage, this degree of agreement may be regarded as sufficient, at least for practical purposes.

Spinodals. Figure 12 shows spinodals calculated with Z given by eq 32 for several values of P and the corresponding experimental data.[3,20,21] Here again, the agreement between calculated and measured values is quite good at any P examined. It is comparable to what was found by Fujita and Teramoto,[6] who adopted an empirical approach to χ very different from ours described in this paper. It should be noted, however, that our expression for χ is free from the physical anomaly involved in theirs.

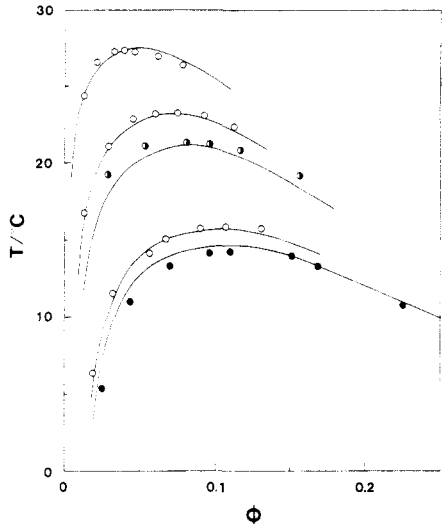

Figure 12. Spinodals for narrow-distribution polystyrene in cyclohexane. Molecular weights of the samples are 520 000, 163 000, 110 000, 51 000, and 43 600 from top to bottom. Open circles, Scholte;[3] closed circles, Ohashi;[20] half-filled circles, Kojima et al.[21] Solid lines show the results from the present calculation.

χ at the Θ Point. The solid lines in Figure 13 illustrate χ_Θ (χ at the Θ point) calculated from eq 32 for four different values of M, and the plotted points indicate measured χ_Θ on the corresponding samples (except for $M = 10^4$).[22] In this range of ϕ, the scatter of the plotted points is greater than or at least comparable with the difference among the upper three curves. Thus, as far as these experimental data are concerned, we will almost surely miss the dependence of χ_Θ on M and conclude that χ_Θ is independent of M. In fact, no previous authors have ever pointed out a molecular weight dependence of χ_Θ. However, the calculated curves in Figure 13 indicate that more accurate measurement should reveal this dependence.

Concluding Remarks

We have shown that our empirical expression for the Flory–Huggins interaction parameter χ is able to predict almost quantitatively critical points, cloud points, and spinodal temperatures for a series of monodisperse polystyrene samples in cyclohexane. No parameter adjustment was made depending on the quantity considered and the sample treated. The success is the outcome not from appropriate modifications of previous theories but from an attempt at describing light scattering data on one-phase solutions as accurately and consistently as possible as a function of T, ϕ, and P. The P dependence of χ_{conc}, among others, is responsible for the achievement of major improvements over previous results. Except at very high molecular weights, this dependence could be revealed by careful and precise experimentation.

As long as no criterion is available for the resolution of χ into χ_{dil} and χ_{conc}, any formulations of χ on the basis of the hybrid theory stand equal, and χ_{conc} in one formulation may contain an appreciable contribution of what is assigned to χ_{dil} in another. Thus, one may criticize that the P dependence of our χ_{conc} is an artifact resulting from the particular type of resolution of χ that was a priori chosen for our data analysis. A relevant answer to this could be obtained from light scattering measurements on solutions of concentrations much higher than those treated in the present work. However, in practice, such measurements are not always feasible, since high viscosities of the solutions make it extremely difficult to prepare uniform test solutions. At any rate, our approach presented in this paper is only an example of a good many other means that can be worked out for a better and deeper understanding of the phase separation phenomenon in strictly binary polymer solutions.

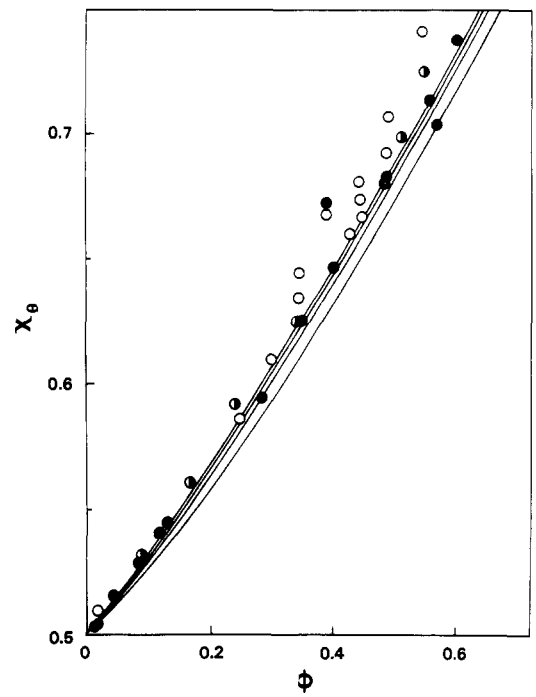

Figure 13. Concentration dependence of χ_Θ for polystyrene in cyclohexane at the Θ point. The experimental points are due to Krigbaum and Geymer.[22] Various marks represent different molecular weight: Open circles, 25 100; half-filled circles, 72 000; filled circles, 440 000. Solid lines indicate χ_Θ calculated by eq 35 for M = 440 000, 72 000, 25 100, and 10 000 from top to bottom.

Registry No. Polystyrene (homopolymer), 9003-53-6; cyclohexane, 110-82-7.

References and Notes

(1) Kurata, M. "Thermodynamics of Polymer Solutions" (translated from the Japanese by H. Fujita); Harwood Academic: New York, 1982.
(2) Koningsveld, R.; Kleintjens, L. A.; Shultz, A. R. *J. Polym. Sci., Part A-2* **1970**, *8*, 1261.
(3) Scholte, Th. G. *J. Polym. Sci., Part A-2* **1971**, *9*, 1553.
(4) Koningsveld, R.; Kleintjens, L. A. *Macromolecules* **1971**, *4*, 637.
(5) Koningsveld, R.; Stockmayer, W. H.; Kennedy, J. W.; Kleintjens, L. A. *Macromolecules* **1974**, *7*, 73.
(6) Fujita, H.; Teramoto, A. In "Proceedings of MMI Symposium on Polymer Compatibility and Incompatibility"; Harwood Academic: New York, 1982; p 125.
(7) Tsuyumoto, M. M.S. Thesis, Osaka University, 1983.
(8) Helfand, E., p 138 of ref 6.
(9) Scholte, Th. G. *Eur. Polym. J.* **1970**, *6*, 1063.
(10) Scholte, Th. G. *J. Polym. Sci., Part A-2* **1970**, *8*, 841.
(11) Koningsveld, R. Thesis, Leiden University, 1967.
(12) We confess that, in formulating this rather complex relation, preliminary data for χ^0_{conc} on other samples were taken into account.
(13) Tong, Z.; Ohashi, S.; Einaga, Y.; Fujita, H. *Polym. J.* **1983**, *11*, 835.
(14) Miyaki, Y.; Fujita, H. *Macromolecules* **1981**, *14*, 742.
(15) Kuwahara, N.; Nakata, M.; Kaneko, M. *Polymer* **1973**, *14*, 415.
(16) Nakata, M.; Kuwahara, N.; Kaneko, M. *J. Chem. Phys.* **1975**, *62*, 4278.
(17) Nakata, M.; Dobashi, T.; Kuwahara, N.; Kaneko, M. *Phys. Rev. A* **1978**, *18*, 2683.
(18) Hashizume, J.; Teramoto, A.; Fujita, H. *J. Polym. Sci., Polym. Phys. Ed.* **1981**, *19*, 1405.
(19) Tsuyumoto, M.; Einaga, Y.; Fujita, H. *Polym. J.*, to appear.
(20) Ohashi, S. B.S. Thesis, Osaka University, 1983.
(21) Kojima, J.; Kuwahara, N.; Kaneko, M. *J. Chem. Phys.* **1975**, *63*, 333.
(22) Krigbaum, W. R.; Geymer, D. O. *J. Am. Chem. Soc.* **1959**, *81*, 1859.